CCFE
CULHAM CENTRE FOR FUSION ENERGY

UK Atomic Energy Authority

UKAEA-CCFE-PR(20)19

D. B. King, E. Viezzer, I. Balboa, M. Baruzzo, E. Belonohy, J. Buchanan, I.S. Carvalho, K. Cave-Ayland, I. Coffey, C.D. Challis, E.G. Delabie, L. Garzotti, S. Hall, J.Hillesheim, L. Horvath, E. Joffrin, D. Keeling, K. Kirov, C.F. Maggi, M. Maslov, S. Saarelma, S. Silburn, E.R. Solano, M. Stamp, D. Valcarcel, H.Weisen

Mixed Hydrogen-Deuterium plasmas on JET ILW

Mixed Hydrogen-Deuterium plasmas on JET ILW

D. B. King, E. Viezzer, I. Balboa, M. Baruzzo, E. Belonohy, J. Buchanan, I.S. Carvalho, K. Cave-Ayland, I. Coffey, C.D. Challis, E.G. Delabie, L. Garzotti, S. Hall, J.Hillesheim, L. Horvath, E. Joffrin, D. Keeling, K. Kirov, C.F. Maggi, M. Maslov, S. Saarelma, S. Silburn, E.R. Solano, M. Stamp, D. Valcarcel, H.Weisen

This is a preprint of a paper submitted for publication in Nuclear Fusion

Mixed Hydrogen-Deuterium plasmas on JET ILW

D. B. King[1], E. Viezzer[2], I. Balboa[1], M. Baruzzo[3], E. Belonohy[1], J. Buchanan[1], I.S. Carvalho[4], K. Cave-Ayland[1], C.D. Challis[1], I. Coffey[5] , E.G. Delabie[6], L. Garzotti[1], S. Hall[1], J. C. Hillesheim[1], L. Horvath[1], E. Joffrin[7], D. Keeling[1], K. Kirov[1], C.F. Maggi[1], M. Maslov[1], S. Saarelma[8], S. Silburn[1], E. R. Solano[9], D. Valcarcel[1], H.Weisen[10]
and JET contributors ‡

Eurofusion Consortium JET, Culham Science Centre, Abingdon, OX14 3DB, UK
[1] Culham Centre for Fusion Energy, Abingdon, UK, [2] Department of Atomic, Molecular and Nuclear Physics, University of Seville, Seville, Spain, [3] Consorzio RFX, Padova, Italy, [4] Instituto de Plasmas e Fusão Nuclear, Instituto Superior Técnico, Universidade de Lisboa, P-1049-001, Lisboa, Portugal, [5] Queens University, Belfast, UK, [6] Oak Ridge National Laboratory, Oak Ridge, USA, [7] CEA, Caderache, France, [8] General Atomics, PO Box 85608, San Diego, CA, 92186-5608, USA [9] Laboratorio Nacional de Fusion, CIEMAT, Madrid, Spain, [10] EPFL, Lausanne, Switzerland

E-mail: damian.king@ukaea.uk

Abstract. A study of mixed hydrogen-deuterium H-mode plasmas has been carried out in JET-ILW to strengthen the physics basis for extrapolations to JET D-T operation and to support the development of strategies for isotope ratio control in future experiments.

Variations of input power, gas fuelling and isotopic mixture were performed in H-mode plasmas of the same magnetic field, plasma current and divertor configuration. The analysis of the energy confinement as a function of isotope mixture reveals that the biggest change is seen in plasmas with small fractions of H or D, in particular when including pure isotope plasmas. To interpret the results correctly, the dependence of the power threshold for access to type-I ELMing H-modes on the isotope mixture must be taken into account. For plasmas with effective mass between 1.2 and 1.8 the plasma thermal stored energy (W_{th}) scales as $m_{eff}^{0.1}$, which is weaker than that in the ITER physics basis, IPB98 scaling.

At fixed stored energy, deuterium-rich plasmas feature higher density pedestals, while the temperature at the pedestal top is lower, showing that at the same gas fuelling rate and power level, the pedestal pressure remains constant with an exchange of density and temperature as the isotope ratio is varied. Isotope control was successfully tested in JET-ILW by changing the isotope ratio throughout a discharge, switching from D to H gas puffing. Several energy confinement times (300 ms) are needed to fully change the isotope ratio during a discharge.

‡ See the author list of "Overview of the JET preparation for deuterium tritium operation with the ITER like-wall" by E. Joffrin et al., Nucl. Fusion 59 112021 (2019)

1. Introduction

Over many years experiments in hydrogen and deuterium across several tokamaks have been run to investigate how thermal energy confinement varies with the fuel isotope mass. Studies were also completed in deuterium-tritium mixtures on TFTR [1] and JET during the DTE1 campaign [2] [3] [4], this being the only time burning plasma relevant experiments were performed. Experiments have been performed in both L-mode and H-mode, with differing results. From these experiments a relatively weak ($\sim M_{eff}^{0.2}$) H-mode confinement scaling with mass has been included in the ITER-98 physics basis [5].

In recent years new studies into isotope effects have begun. This has been motivated by the need for ITER operations in the non-nuclear phase in different isotopes, the upcoming DT campaign on JET and the validation of new modelling tools. Experiments were carried out on JT-60U [6], [7], [8], ASDEX Upgrade [9], [10], [11] and on JET with the ITER Like Wall (ILW) [12], [13], [14].

However, the behaviour of mixed isotope plasmas is less well understood due to fewer studies, particularly in machines with metal walls. During previous DT studies (conducted in carbon wall machines) the experiments mainly used 50:50 isotope mixtures and did not have systematic studies using varying isotope mixtures. A study of hydrogen-deuterium (H-D) H-mode plasmas in JET-ILW strengthens the physics basis for extrapolations to JET deuterium-tritium (D-T) operation, supports the development of strategies for isotope ratio control for the future D-T campaign and provides stringent tests for plasma transport models. Beyond JET the fuelling behaviour of mixed isotope plasmas and the behaviour of hydrogen majority plasmas is relevant for ITER operations.

Experiments in mixed H-D plasmas have been performed on JET to study the effect of isotope composition on plasma properties, in particular the H-mode confinement. This work is part of a wider study of the isotope effect on JET including the confinement of pure hydrogenic plasmas [12] and the effect of isotope on the L-H transition in [13]. A summary of the JET-ILW campaign can be found in [15].

2. Experiment

The experiment reported here involved carrying out scans of the isotope mixture ($n_H/(n_H + n_D)$) in similar, stationary plasmas (stable for several energy confinement times) and is supported by scans of input power and gas fuelling. The isotope mixture was varied from 1.05 <M_{eff}<1.8 with an increased number of pulses performed near M_{eff}=1.0 to examine if there were significant effects at marginal levels of the

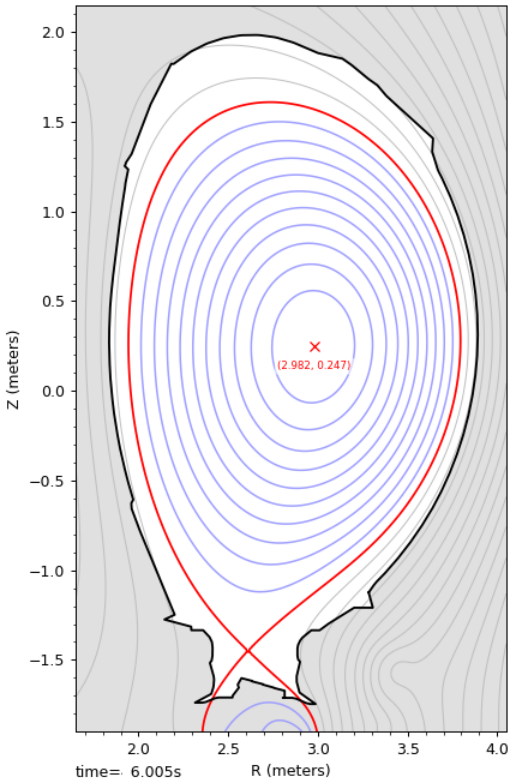

Figure 1: *Equilibrium of plasma used in experiment. Pulse 91215 at 6.005s*

minority isotope [16]. The scans were performed in type-I ELMy H-mode plasmas of fixed plasma current (1.4 MA), toroidal magnetic field (1.7 T), total gas fuelling rate (1-1.1x10^{22} el/s) and plasma shape as shown in Figure 1 (with strike points in the corner of the divertor where pumping is more effective). Plasma heating was provided predominantly by neutral beam injection of either deuterium or hydrogen up to a maximum injected power of 14 MW but with most plasmas in the range of 8-10 MW. When only hydrogen NBI was available the maximum power was 8-10MW. For these plasma parameters ($B_T = 1.7T$) the L-H power threshold for a pure hydrogen plasma is expected from similar JET pulses to be 9-10MW [13].

These parameters were chosen so that comparisons could be made with other, pure isotope experiments carried out during the same experimental campaigns [12]. While the isotope mixture scans discussed above did not include pure H or D plasmas, it was possible to compare the data to type-I ELMy H-mode data from pure isotope experiments reported in [12] to complete the full range of the isotope ratio scan.

In H-mode plasmas the confinement, ELM frequency and pedestal behaviour are strongly affected by the input power and the gas fuelling level used. To attempt to characterise these relationships in a

mixed isotope plasma the input power and gas fuelling level were both varied in plasmas with a 50/50 isotope ratio. The plasma responded as expected with these variations, with ELM frequency increasing with increased power and gas. The range of power and gas fuelling tested was 8-14 MW for the power (NBI heating) and 5-12x10^{21} el/s for the gas fuelling.

2.1. Isotope Ratio Measurements

In order to carry out experiments of this nature it is necessary to accurately measure the isotope ratio. For comparison, a description of the diagnostics used during the DTE1 campaign can be found in [17]. On JET there are a number of diagnostics that measure the H/D ratio at the edge of the plasma but no direct measurement of the ratio in the plasma core was available for this experiment. The edge ratio is measured spectroscopically and with sub-divertor gauges. The spectroscopy technique involves comparing the relative amplitude of Balmer H_α/D_α spectral lines from the plasma edge measured by high resolution spectrometry with lines of sight viewing the inner and outer divertor. The sub-divertor neutral gas pressure is measured by the spectral analysis of H_α (D_α) emission from a penning gauge discharge. These two measurements typically agree well with each other (within $< 5\%$).

As there is no core isotope ratio measurement available a technique was developed to estimate the core isotope mixture via the relationship between the neutron rate and core deuterium content. Neutrons are produced in these pulses by thermal D-D reactions and fast, D NBI generated ions with the background D plasma, the latter being the larger reaction in these plasmas. Reactions take place predominantly in the plasma core with the beam target reactions being roughly proportional to the deuterium density ($n_D/(n_D+n_H)$ for the dilution effect with an additional effect due to the isotope dependence of the fast ion slowing down time. The resulting dependence is demonstrated in the curve shown in Fig. 3.

The first step in this calculation is to run TRANSP simulations [18] for a set of pure D reference plasmas in similar conditions as the mixed isotope experiments. This is necessary to quantify the discrepancy between measured and calculated neutron rates, which is typically found on JET [19], for this set of plasmas. A key assumption in the method is that any discrepancy in the neutron rate is consistent for the relevant plasma parameters over a range of H/D ratio.

Pure D reference plasmas were taken from both the 2013 and 2014 JET campaigns, 3 pulses from each campaign [12]. The plasma current, toroidal field, NBI power, Z_{eff}, average density and temperature were similar to the plasmas used in this experiment. TRANSP simulations were performed with fitted profile data from high resolution Thomson scattering (HRTS) and core Thomson scatting (LIDAR) for electron density and temperature, charge exchange recombination spectroscopy (CXRS) for toroidal rotation and ion temperature, horizontal visible bremsstrahlung for Z_{eff}, assuming beryllium as the sole impurity, and using the TRANSP internal equilibrium solver. The simulations were repeated with $T_i = T_e$ to estimate the error from the ion temperature (typically very close to electron temperature in these plasmas).

For all of the pulses analysed the modelled neutron rate was $\sim 20\%$ higher than the measured neutron rate, R. Using the measured ion temperature data the average over pulses gave $R_{modelled}/R_{measured} = 1.19$ with a standard deviation of $\sigma = 0.06$ while using $T_i = T_e$ gave $R_{modelled}/R_{measured} = 1.21$ with $\sigma = 0.07$. Simulations were repeated using the EFIT equilibrium to quantify errors due to profile fitting, this only changed the modelled neutron rate by $\sim 3\%$. These neutron discrepancies are consistent with those reported in [19].

Following this, TRANSP runs were performed using the same input and model assumptions on mixed isotope plasmas of interest for a range of isotope ratios with the modelled neutron rate renormalised to take account of the discrepancy found above. This normalisation compensates for systematic modelling and measurement errors. Any remaining neutron discrepancy is considered to be caused by the level of hydrogen assumed in each simulation. This discrepancy is fitted against isotope ratio at a particular time and then that fit is used to calculate an isotope ratio that agrees with the neutron rate at each time point. The fit used is quadratic rather than linear as there is also a dependence of fast ion slowing down time on ion mass.

This method was used on pulse 91274 where gas fuelling changes from D to H during the pulse and 30% of beam fuelling is from H beams, see Figure 2. The plot also shows the edge isotope ratio representative of the outer divertor region. The fit of $R_{modelled}/R_{measured}$ vs n_D used for this pulse is shown in Figure 3.

The error in the neutron rate modelling calculated above translates to only a $\sim$ 3% error in the D concentration because of the non-linear fit in Figure 3. This is the error that has been possible to calculate but does not exclude the possibility of other errors in the isotope ratio and neutron modelling, particularly as the cause of the neutron discrepancy on JET and other devices is not known. However, given the consistency in comparison with pure D plasmas any further errors are not expected to be large. It should also be noted that the D concentration calculated using

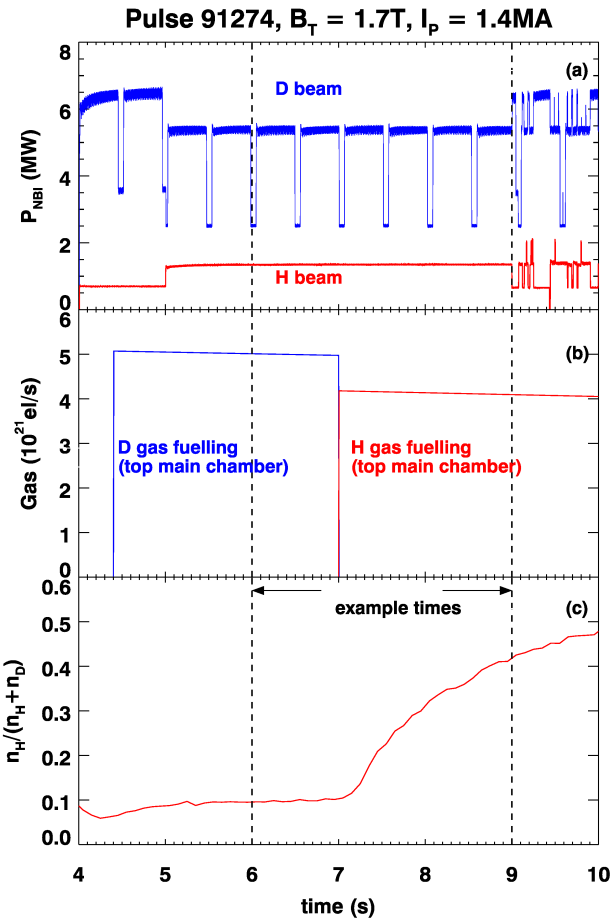

Figure 2: *NBI power, gas fuelling and edge isotope ratio for JET pulse 91274. Note that drops in NBI power are intentional to provide charge exchange data.*

this method represents the region of plasma where neutron production takes place, which is primarily in the core of the plasma. In pulse 91274 for example, the TRANSP calculations show that $\sim 50\%$ of neutrons are generated within $\rho = 0.3$ and $\sim 90\%$ of neutrons are generated within $\rho = 0.6$. Results of this core isotope ratio analysis will be used in plots in the subsequent sections of this paper.

2.2. Isotope Ratio Control

On fusion devices such as JET the fuelling actuators are gas puffing through gas introduction modules in both the main chamber and divertor, NBI and pellets. Wall recycling also acts as a source/sink of gas. The JET device has a cryo-pump located in the divertor region, the pumping efficiency of which will also vary with isotope. For the pulses discussed here pellet fuelling was not used. In machines with metallic walls the recycling is significantly reduced compared to the recycling in carbon wall machines, including earlier

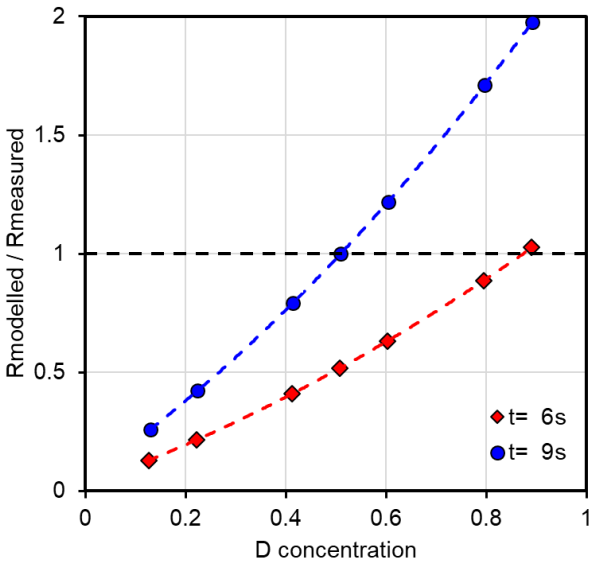

Figure 3: *Ratio of modelled to measured neutron rate vs D concentration for JET pulse 91274. The timepoints are indicated by the dashed lines in figure 2.*

experiments on JET while it had a carbon wall. While there is some legacy effect of the isotope present in the wall, this is typically small [20]. NBI can be a significant fuelling source at the core of the plasma and this experiment aimed to demonstrate effects of beam isotope on the plasma and how much of an effect this had on the core isotope ratio. It has been shown that NBI fuelling does not significantly change the core isotope ratio in these plasmas [21]. Similar results were found in [17] but with significant uncertainty.

The isotope injected using gas puffing was the control actuator used throughout the experiment. Gas can be fuelled on JET from a number of locations in the main chamber and in the divertor region. Two similar gas dosing locations (described in each figure where relevant) were chosen for the fuelling during the main heating phase of the pulse, one in H and the other in D. By varying the pressure in the system and the valve opening the amount of H and D introduced can be varied. For pulses with constant gas dosing the relative amounts of H and D required was pre-programmed in feed-forward control. Feedback control was also used with the Balmer-Alpha diagnostic described above used to control the relative opening of H and D valves.

The effectiveness of the feedback mechanism is shown in Figure 4. The gas fuelling from hydrogen and deuterium varies in response to the measurement maintaining $n_H/(n_H+n_D) \sim 0.5$ for a range of injected power. The data in Figure 4(c) also shows that the core isotope ratio is the same as the edge isotope ratio within the errors of the core estimate.

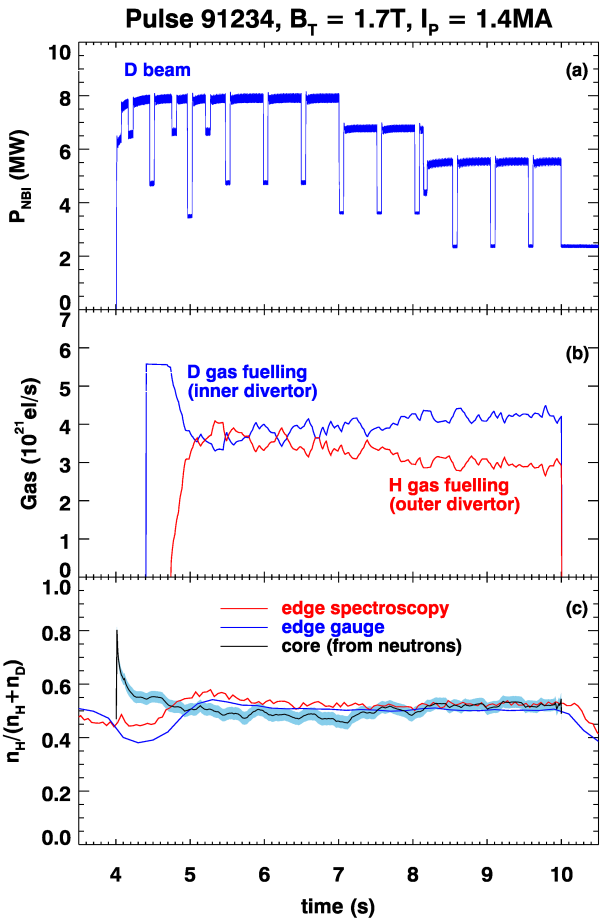

Figure 4: *Real time control of isotope ratio in edge and core. Estimated error in core isotope ratio represented by shaded region.*

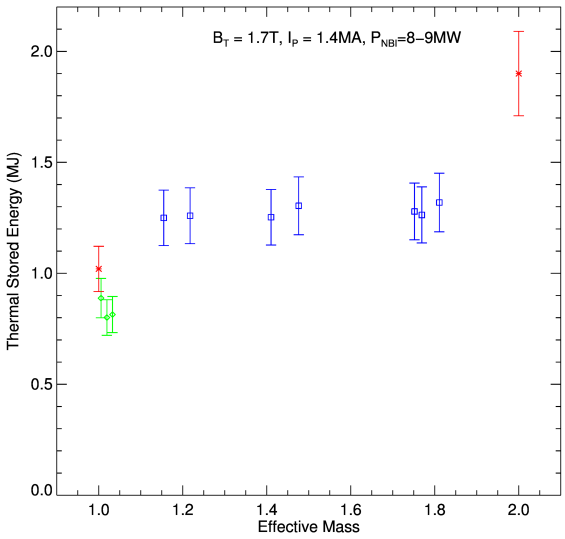

Figure 5: *Thermal stored energy calculated by TRANSP vs effective mass for mixed isotope plasmas (blue) including plasmas with very low deuterium content (green) and pure isotope plasmas (red)*

3. Energy Confinement Dependence on Isotope Ratio

To determine the effect of isotope ratio on energy confinement the plasma thermal stored energy (W_{th}) at constant input power can be compared for different values of M_{eff}. Given the effect of gas fuelling rate on the ELM behaviour, pedestal height and plasma performance it is important that pulses with the same total gas fuelling rate be used in any such comparison. The W_{th} was calculated in two different ways. The kinetic profiles can be integrated to calculate a W_{th}. This was done as part of interpretive TRANSP [18] calculations. Diamagnetic measurements of stored energy can also be used if they are corrected for the fast particle fraction of stored energy calculated by PENCIL [22]. The error bars in W_{th} and τ_e shown in Figures 5 and 6 represent the difference between these two calculation methods.

Pulses were successfully carried out for a range of isotope ratios with 8-9 MW of input power and gas

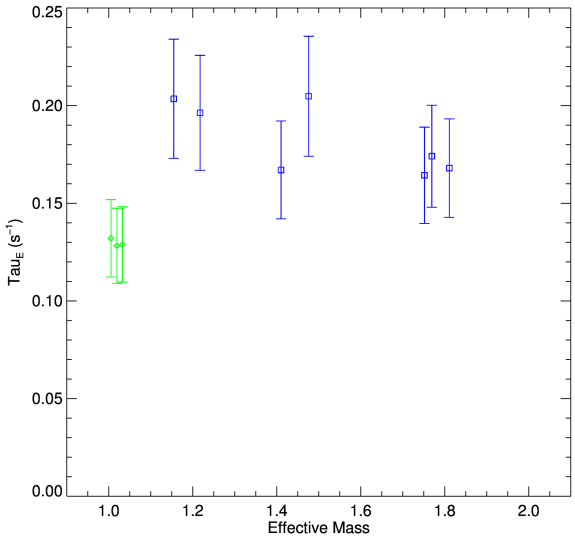

Figure 6: *Thermal energy confinement time calculated by TRANSP vs effective mass for mixed isotope plasmas (blue) including plasmas with very low deuterium content (green)*

fuelling rate of 1-1.1x10^{22} el/s. The data shows the appearance of a complex dependence on isotope ratio. The energy confinement, through W_{th}, as a function of the effective mass is shown in Figure 5. Variations in input power have been examined in these pulses and the change in ELM frequency with power show that they are in type-I ELMy H-mode. Analysis of the power footprint in the divertor using IR data also indicates that the pulses are in type-I ELMy H-mode due to variations in power width between type-I and type-III ELMs. The data in Figure 5 shows that there is no significant dependence of confinement on isotope mixture for the blue points.

As the L-H power threshold increases when going to H plasmas, for the pulses with 1.0 <M_{eff}<1.1 it was not possible to determine if the pulses were in type-I or type-III ELMy H-modes (green stars) so they are represented differently. If these pulses are included they show that a stronger dependence on isotope ratio is present and appears to be important near the pure isotope point. Finally, if data from the pure isotope ratio experiments [12] are included, as the red points in Figure 5 then the stronger isotope dependence at low H and D concentrations is clearer.

The confinement time for the thermal stored energy has also been calculated using TRANSP, the dependence of this on effective mass is shown in Fig. 6. This data shows the same behaviour as the thermal stored energy with no clear dependence on isotope ratio for 1.1 <M_{eff}<1.8 but with a larger variation in the pulses with M_{eff}<1.1.

It has been shown that the L-H power threshold has a non-linear isotope ratio dependence [13] with large changes in P_{L-H} at very low minority concentrations. As the pulses involved were carried out at power levels close to P_{L-H} it is possible that the confinement dependence on isotope mixture in Figure 5 is a manifestation of the changes in P_{L-H}. To further investigate this further experiments at higher input power are necessary.

4. Pedestal

Comparison of pure D and H plasmas showed that at constant gas fuelling rate and power input the pedestal pressure in H is lower than in D [12]. This is in agreement with results from ASDEX Upgrade, where pedestal matching experiments in D and H showed that in order to achieve the same pedestal height in density and temperature more gas and more power, respectively, are needed in H [10]. Similarly, on JT-60U it was observed that the temperature pedestal is higher in D compared to H in H-mode plasmas with similar absorbed power, while the pedestal density stays the same in both D and H [23].

The impact of changing the isotope ratio on the pedestal structure was analyzed for the same subset of pulses where the isotope ratio was scanned at constant total gas fuelling rate (1-1.1 $\times$ 10^{22} el/s), as presented in the previous section. Only discharges with NBI heating at a similar power level (8–9 MW) were included. The measured electron density and temperature profiles were fitted with a modified hyperbolic tangent function [24]. Note that the ELM-averaged profiles are used for the analysis as the ELM frequency across the scan was too high.

Figure 7 shows the electron density and temperature at the pedestal top (taken at $\rho_{pol} = 0.95$) as a function of the effective mass. As shown, at constant gas fuelling rate, the D-rich plasma features a higher density pedestal. This indicates that in H, or in plasmas with H majority, a much larger gas puff is needed to reach the same pedestal density, consistent with results from ASDEX Upgrade [10] and with the pure isotope experiments [12]. The temperature shows the opposite trend, i.e. D-rich plasmas feature lower values of T_e at the pedestal top, indicating that at constant gas and power the density decreases and temperature increases to maintain a constant pressure as the isotope ratio is varied from H-rich to D-rich plasmas.

Figure 8 shows the n_e-T_e diagram for this subset of data. As the isotope ratio changes from predominantly D (H/(H+D) < 0.3) to predominantly H (H/(H+D) > 0.75) the datapoints move along isobars, exchanging density and temperature. This is consistent with the findings in full D and full H plasmas [12].

5. Isotope Exchange

To determine the rate at which the core and edge isotope ratio could vary a discharge was performed where the gas fuelling was switched from D to H during the type-I ELMy H-mode phase, while other parameters were kept the same as in the isotope ratio scan. This test was performed with both divertor and main chamber gas fuelling. It can be seen in Figure 9 and 10 that in both cases the core isotope ratio closely follows the edge isotope ratio, this agrees with [25] and [26]. Comparing Figures 9 and 10, the core isotope ratio appears to change more rapidly in the main chamber fuelling case indicating a higher fuelling efficiency but this could also be due to the proximity of the diagnostic to the divertor gas puff. This pulse also contains 20% H NBI power so the difference could either be related to diagnostic, gas fuelling position or beam fuelling. It takes $\sim$ 10 energy confinement times (calculated from TRANSP runs performed as above [18]) for the plasma composition to change from $\sim$ 5% to $\sim$ 50% $n_H/(n_H + n_D)$.

When changing gas species within the discharge

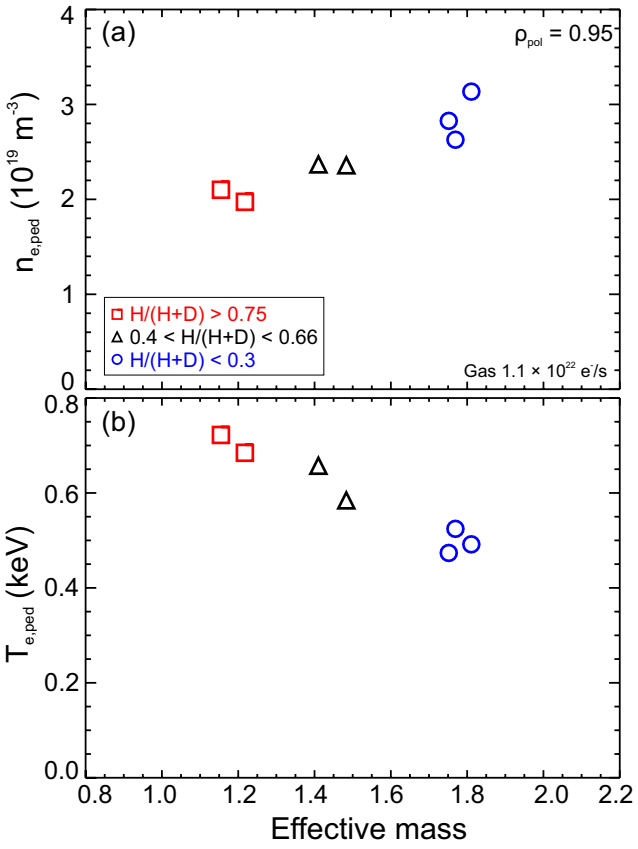

Figure 7: *Pedestal electron density (a) and temperature (b) (taken at $\rho_{pol} = 0.95$) as a function of the effective mass.*

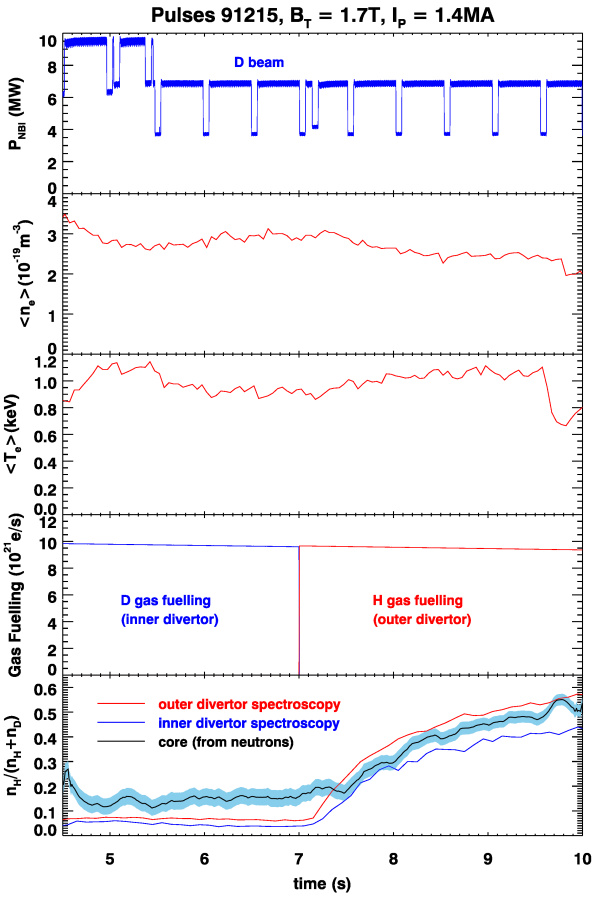

Figure 9: *Change in isotope ratio with gas fuelling using divertor fuelling. Estimated error in core isotope ratio represented by shaded region.*

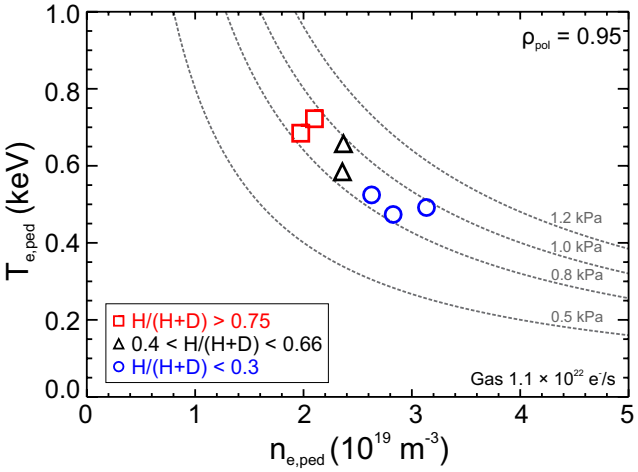

Figure 8: *Pedestal density and temperature for pulses across range of isotope ratio and pure isotope pulses across a range of input power and gas fuelling.*

the change in plasma behaviour is much faster than the change in overall plasma composition. This is exemplified in Figure 11, which shows the ELM behaviour (from Beryllium emission) when the gas isotope is changed. The valve response is 100ms and within 200ms of the gas switch from D to H the ELM frequency changes from 70Hz to 50Hz. This could either be related to the small change in isotope ratio having a large effect (as on confinement) or the effect of neutral penetration acting more quickly on the ELM behaviour.

Previous results have shown that the ELM frequency decreases with isotope mass [2] but in Figure 11 the ELM frequency is higher with D gas fuelling. The contradictory reduction in ELM frequency in H seen in Fig. 11 can be explained by the effect of the lower isotope mass on the L-H threshold power. As the hydrogen concentration begins to increase the L-H power threshold increases. As the ELM frequency also increases with input power above threshold this could

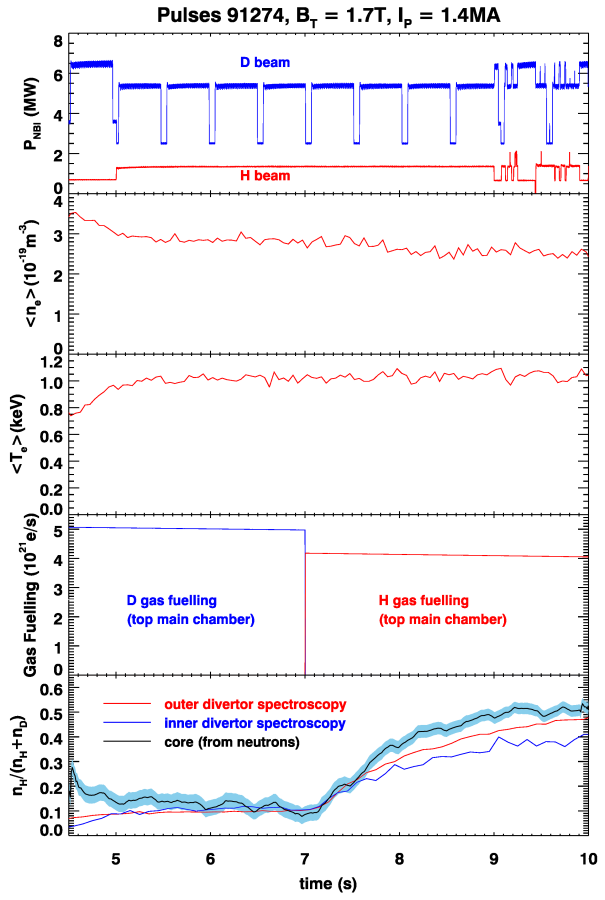

Figure 10: *Change in isotope ratio with gas fuelling using main chamber fuelling. Estimated error in core isotope ratio represented by shaded region.*

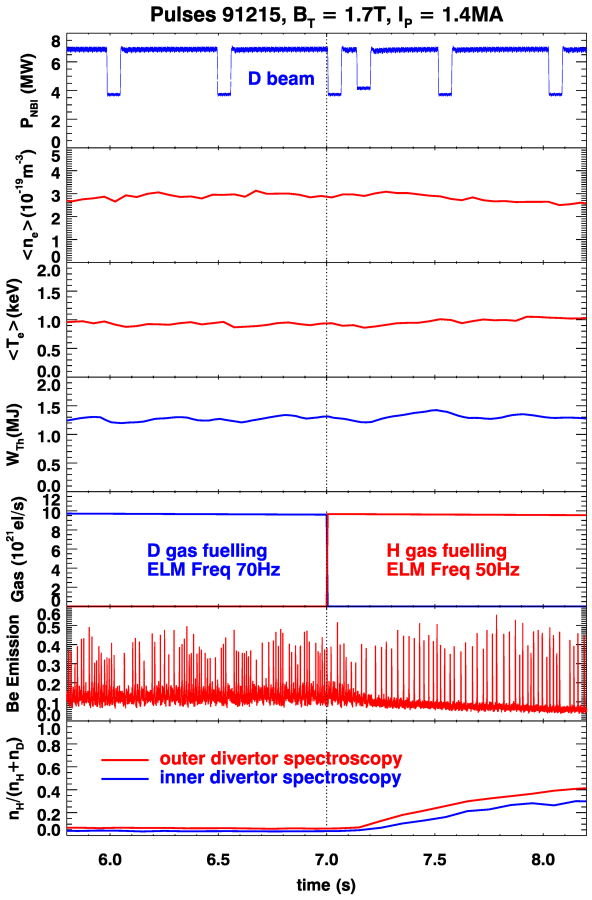

Figure 11: *Effect of change in gas fuelling on stored energy, isotope ratio and ELM behaviour.*

cause the drop in ELM frequency within this pulse.

The density and temperature profiles have been examined from periods before and after the gas fuelling change above, these profiles are shown in Figure 12. In agreement with the results shown in section 4 the pedestal density is higher in the deuterium fuelled case while the pedestal temperature is lower. Also, it is clear that the density peaking of the deuterium plasma is lower than for the hydrogen plasma, however this could be related to the lower density pedestal leading to increased core beam fuelling. Density peaking due to core sources and transport has been the subject of many studies and the relative contribution remains uncertain, requiring further investigation and more experiments [27], [28], [29] . Modelling has shown that there is a weak effect of isotope mass on density peaking but this was in plasmas without NBI heating, so there was no central source of particles [30]. The effect of isotope mass on density peaking is subject to future work and should be considered for JET DT plasmas.

6. Conclusions

It has been shown that the plasma confinement in mixed H/D plasmas does not vary significantly with isotope ratio between $1.2<M_{eff}<1.8$. There is a more significant change in confinement at very low minority concentrations (consistent with [12]), this is also supported by the change in ELM frequency for small change in isotope ratio in the pulse with changing gas fuelling. As the fuelling is changed from D to H, the ELM frequency decreases. This is most likely attributed to the change of the L-H power threshold as the plasma transits from more D-content to a more H-rich plasma. To disentangle the effects on the ELM frequency from the L-H power threshold, more experiments at higher input power are required. Due to the proximity to the L-H power threshold (expected from similar JET pulses to be 8-9MW for pure hydrogen at these parameters) it is still unclear

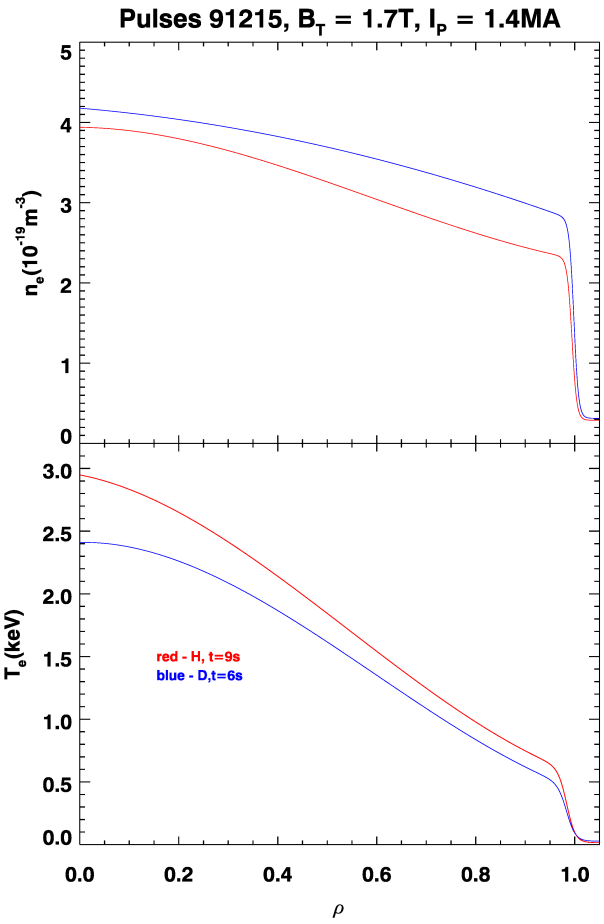

Figure 12: *Density and temperature profiles of deuterium and hydrogen fuelling phases of pulse 91215 fitted to HRTS data.*

whether the stored energy variation is a change in the confinement behaviour directly or due to the changes in L-H power threshold as seen in [13].

Across isotope mixtures, at fixed stored energy, the pedestal density decreases while the pedestal temperature increases thus, maintaining constant pressure. Deuterium rich plasmas are observed to be colder and more dense. This is consistent with the edge properties of pure H vs D plasmas [12]. This result is of particular interest for upcoming DT experiments on JET, as it shows the importance of achieving the appropriate isotope mixture on plasma performance. Other parameters such as ELM frequency (controlled by gas fuelling level or pellet pacing) will also affect the pedestal temperature in DT but they may be determined by other constraints (such as control of impurity accumulation), so the ability to compensate for a lower pedestal temperature may be limited. Given the relationship between density peaking and impurity accumulation the difference in the density profiles for different isotope ratios is of particular interest for JET-DT.

The strong effect of small amounts of minority isotopes on energy confinement shows how it is vital for isotope studies to be carried out at high isotope purity. Previous studies comparing plasmas of hydrogen, deuterium and tritium in JET-C may not have achieved this level of purity. Indeed, the isotope studies performed on JET with the carbon wall (where high isotope purity is more difficult to achieve) [2] typically had $\leqslant 95\%$ isotope purity.

It has been demonstrated that isotope control in JET ILW can be successfully performed and that many confinement times would be required to fully change the isotope ratio within the same discharge. This could have consequences for potential burn-control methods on fusion reactors. Finally, it has been shown that the core isotope composition of these pulses is primarily determined by the isotope of the gas fuelling with beam fuelling only having a small effect, as demonstrated in more detail in [21]. This could depend on SOL opacity, so the extrapolation to ITER is not yet clear.

Further experiments in H-D at higher input power and plasma current would allow more reliable extrapolation to higher performance JET-ILW plasmas and to larger plasmas such as in ITER. Experiments at higher power, including a scan of NBI power at high H concentration, would also help to separate the effects of L-H threshold from those of confinement. The study could also be extended to H-T mixtures on JET in further preparation for the upcoming D-T campaign.

This work has been carried out within the framework of the EUROfusion Consortium and has received funding from the Euratom research and training programme 2014-2018 and 2019-2020 under grant agreement No 633053 and from the RCUK Energy Programme [grant number EP/I501045]. The views and opinions expressed herein do not necessarily reflect those of the European Commission. The support from the H2020 Marie-Sklodowska Curie programme (Grant No. 708257) and the Spanish Ministry of Economy and Competitiveness (Grant No. FJCI-201422139) is gratefully acknowledged.

7. References

[1] Scott, S.D et al. in Fusion Energy 1996 (*Proc. 16th Int. Conf. Montral 1996*) Vol. **1** p. 573-590, IAEA, Vienna, (1997)
[2] Saibene G et al. 1999 *Nucl. Fusion* **39**, 1133 [2]
[3] Cordey J.G et al. 1999 *Nucl. Fusion* **39**, 301 [3]
[4] Righi E et al. 1999 *Nucl. Fusion* **39** 309
[5] ITER Physics Basis Expert Groups on Confinement and Transport and Confinement Modelling and Database, ITER Physics Basis Editors, 1999 *Nucl. Fusion* **39** 2175
[6] Urano H et al. 2008 *Nucl. Fusion* **48** 045008
[7] Urano H et al. 2012 *Phys. Rev. Lett.* **109** 125001
[8] Urano H et al. 2013 *Nucl. Fusion* **53** 083003

[9] Schneider P et al. 2017 *Nucl. Fusion* **57** 066003
[10] Laggner F M et al. 2017 *Physics of Plasmas* **24**, 056105
[11] Viezzer E et al. 2018 *Nucl. Fusion* **58**, 026031
[12] Maggi C F et al. 2018 *Plasma Phys. Control Fusion* **60** 014045
[13] Hillesheim J et al. 2017 *44th EPS Conf. on Plasma Physics, Belfast* P5.162
[14] Delabie E et al. 2017 *44th EPS Conf. on Plasma Physics, Belfast* P4.159
[15] Litaudon X. et al. 2017 *Nucl. Fusion* **57** 102001
[16] King et al. 2017 *44th EPS Conf. on Plasma Physics, Belfast* O3.112
[17] Maas A C et al. 1998 *20th Symposium on Fusion Technology, Marseille* **1** 693
[18] Goldston R J et al. 1981 *J. Comp. Phys* **43** 61
[19] Weisen et al. 2017 *Nucl. Fusion* **57** 076029
[20] Brezinsek S. et al. 2013 *Nucl. Fusion* **53** 083023
[21] Maslov M et al. 2018 *Nucl. Fusion* **58** 076022
[22] Challis C D et al. 1989 *Nucl. Fusion* **29** 563
[23] Urano H. et al. 2012 *Nucl. Fusion* **52** 114021
[24] Groebner R. J. et al. in Fusion Energy 1996 (*Proc. 16th Int. Conf. Montral 1996*) Vol. **1** p. 867-873, IAEA, Vienna, (1997)
[25] Bourdelle C. et al. 2018 *Nucl. Fusion* **58** 076028
[26] Marin M. et al. 2020 *Nucl. Fusion* **60** 046007
[27] Valovic M. et al. 2007 *Nucl. Fusion* **47** 196
[28] Garzotti L. et al. 2006 *Nucl Fusion* **46** 994
[29] Tala T. et al. 2019 *Nucl. Fusion* **59** 126030
[30] Angioni C. et al. 2018 *Physics of Plasmas* **25** 082517